Effects of Solute Concentration on Equilibrium Partitioning of Flexible Macromolecules in Fibrous Membranes and Gels

Jeffrey A. White[†] and William M. Deen*[,†,‡]

Department of Chemical Engineering and Division of Bioengineering and Environmental Health, Massachusetts Institute of Technology, Cambridge, Massachusetts 02139

Received December 27, 2000; Revised Manuscript Received June 8, 2001

ABSTRACT: A theory was developed to describe the equilibrium partitioning of flexible, linear polymers between a concentrated polymer solution and a medium consisting of a randomly oriented array of fibers (e.g., a fibrous membrane or gel). The fibers were represented as long cylinders, and the solute was modeled as a chain of cylindrical segments joined at specified bond angles. A Monte Carlo technique combined with excluded-volume concepts was used to describe steric interactions among chains and between chains and fibers. The partition coefficient (Φ, the solute concentration in the fibrous material divided by that in the bulk solution) was predicted to increase markedly when the bulk solution concentration of the polymer was elevated. This sensitivity of Φ to bulk concentration was found even at concentrations that were well below critical overlap values. The predicted partition coefficient decreased significantly as fiber volume fraction or molecular size was increased but tended to be less sensitive to the structural details of the chain (segment number, segment radius, and bond angle). Partition coefficients for dextran in agarose gels were measured as a function of agarose volume fraction, dextran size, and dextran concentration. The trends in the data were in good agreement with the theory. Over the range of dextran concentrations studied, as much as a 5-fold increase in Φ was observed.

Introduction

The equilibrium distribution of macromolecules between a solution and a gel or fibrous medium is important in size-exclusion chromatography, membrane-based separation processes (e.g., ultrafiltration), and the transport of large molecules through body tissues, among other applications. This equilibrium is characterized by the partition coefficient

$$\Phi = \frac{\bar{C}}{C} \tag{1}$$

where $\bar{C}$ is the solute concentration in the fibrous phase (based on total volume, including solids) and C is the concentration in the adjacent solution. (Overbars are used throughout to denote quantities evaluated in the fibrous phase.) Fibrous materials and polymeric gels frequently have disordered structures, which suggests that they be modeled as arrays of randomly oriented fibers with fluid-filled interstices. To a first approximation, these fibers can be viewed as rigid, infinitely long cylinders of uniform cross section. The partitioning of dilute solutions of spherical molecules in such media was analyzed originally by Ogston.[1] A restriction to very dilute solutions is necessary to justify the neglect of solute−solute interactions. Such interactions were considered by Fanti and Glandt[2] for solutions of uniform spheres and by Lazzara et al.[3] for arbitrary shapes, including mixtures of unlike spheres and/or oblate or prolate spheroids. For concentrated solutions with a single type of solute, steric interactions among solute molecules were always found to increase Φ, sometimes markedly.

There are few theoretical results for the partitioning of flexible polymers in disordered media. Thompson and Glandt[4] used an integral equation method to analyze the partitioning of a polymer (represented as a chain of hard spheres) in a medium consisting of a random array of nonoverlapping spheres. As with rigid solutes, the partition coefficient was found to increase with the polymer concentration. We previously used a Monte Carlo technique to model the partitioning of dilute solutions in random fiber arrays, in which the polymers were represented as chains of $n - 1$ line segments joining n mass points.[5] Partition coefficients were computed by generating an ensemble of chain configurations and determining the probability of successfully fitting a chain in a given fiber matrix. Results were obtained both for random-flight chains and for chains with a fixed bond angle between neighboring segments.

The objective of the present study was to predict values of Φ for concentrated solutions of flexible polymers in media consisting of randomly oriented fibers. This extension of our previous work required the introduction of a parameter related to the volume occupied by a polymer chain. Chains of mass points joined by line segments cannot interact sterically with each other because they have no solid volume. Although it has been suggested that such a chain be assigned a volume corresponding to that of the smallest convex object that would enclose it,[6] this might greatly overestimate the actual excluded volume for pairs of chains. Alternative representations include a chain composed of hard spheres and one where each segment is a cylinder of uniform radius; we adopted the latter model. Partition coefficients were computed by combining the excluded-volume methodology of Lazzara et al.[3] with a Monte Carlo technique. To test the predictions, experimental results were obtained for the partitioning of dextrans in agarose gels. An advantage of agarose is that it forms hydrogels that exhibit little or no osmotic

[†] Department of Chemical Engineering.
[‡] Division of Bioengineering and Environmental Health.
* Address for correspondence: Telephone (617) 253-4535, Fax (617) 258-8224, E-mail wmdeen@mit.edu.

10.1021/ma0022046 CCC: $20.00
Published on Web 10/04/2001

swelling or shrinkage, making gel volume independent of the dextran concentration. After the modeling methodology and experimental procedures are described, general results are presented to illustrate the effects of radius of gyration, segment radius, segment number, bond angle, fiber radius, and fiber volume fraction on partitioning. The predictions are then compared with the data and the strengths and limitations of the theory are discussed.

Model Formulation and Computational Methods

Overall Formulation. The fibers in the membrane or gel were modeled as straight, infinitely long cylinders of radius r_f, with random orientations. Macromolecular solutes were represented as chains consisting of n mass points joined by $n - 1$ cylindrical segments, each of length l and radius r_c. The segments were allowed to rotate freely at a fixed bond angle, β, defined such that $\beta = 0$ for a chain that doubles back on itself and $\beta = 180°$ for a fully extended rod. The radius of gyration (r_g) of the chain was related to the other parameters by[7]

$$r_g = \frac{l}{n}\{\sum_{j=1}^{n}\sum_{i=1}^{j-1}[j - i + 2\sum_{k=1}^{j-i-1}(j - i - k)(-\cos\beta)^k]\}^{1/2} \quad (2)$$

In the calculations, r_g, n, and β were used as the independent variables, and the corresponding value of l was computed using eq 2.

With only steric interactions assumed to be present, the equilibrium partition coefficient is the probability that a solute molecule (flexible chain) will avoid overlaps with other objects (fibers or chains) in the fiber or gel phase, relative to the probability that it will avoid overlaps in an equivalent volume of bulk solution. In computing those probabilities, it is necessary to sample all positions within the respective test volumes as well as all possible chain orientations and conformations. Thus, the partition coefficient is a ratio of configuration integrals.[8] To obtain a computationally tractable problem, all fibers and chains were approximated as independent (and potentially interpenetrating) objects. When applied to analogous calculations of partition coefficients for rigid solutes at finite concentration, this relatively simple approach has been shown to give results that are in good agreement with other methods.[3] An important simplification is that it allows chain−fiber and chain−chain interactions to be considered separately. Moreover, interactions among pairs of chains are considered to be the same, on average, in both phases. That is, any tendency of the fibrous medium to select certain chain conformations is neglected. The analysis of chain−fiber interactions was very similar to that described in a recent model of partitioning in dilute solutions.[5] Likewise, the treatment of chain−chain interactions in terms of excluded volumes closely paralleled that used recently for rigid solutes.[3] The difference in the excluded-volume model is that, whereas there are explicit analytical expressions for the excluded volumes between simple objects such as spheroids,[6] the excluded-volume parameter needed here had to be computed numerically, using a Monte Carlo approach to do the positional, orientational, and conformational sampling.

The probability of there being no overlap (shared solid volume) between a test chain and other chains in the bulk solution is denoted as P_{cc}, and the probabilities of no overlaps with fibers or other chains in the fibrous phase are $\bar{P}_{fc}$ and $\bar{P}_{cc}$, respectively. It follows from the assumption of independent interactions that

$$\Phi = \frac{\bar{P}_{fc}\bar{P}_{cc}}{P_{cc}} \quad (3)$$

The partition coefficient for an arbitrarily dilute solution is denoted as $\Phi^{(0)}$. With solute−solute interactions negligible, $P_{cc} = \bar{P}_{cc} = 1$ and $\Phi = \Phi^{(0)} = \bar{P}_{fc}$. This allows eq 3 to be rewritten as

$$\Phi = \Phi^{(0)}\frac{\bar{P}_{cc}}{P_{cc}} \quad (4)$$

Another consequence of the assumption of independent interactions is that the probability of a given number of intersections between the test chain and other chains follows a Poisson distribution.[3] Accordingly, for a solution of chains with number concentration C, the probability of no overlaps is

$$P_{cc} = \exp(-CV) \quad (5)$$

where V is the configuration-averaged excluded volume for a pair of chains. That is, CV is the fraction of the total volume excluded to an arbitrary chain. Similarly, $\bar{P}_{cc}$ is given by

$$\bar{P}_{cc} = \exp(-\bar{C}V) \quad (6)$$

Relating $\bar{C}$ to C using the partition coefficient, eq 4 becomes, finally,

$$\Phi = \frac{\Phi^{(0)}}{P_{cc}^{\,1-\Phi}} \quad (7)$$

Given values of $\Phi^{(0)}$ and P_{cc}, this implicit expression for Φ was solved using Newton−Raphson iteration. The evaluation of $\Phi^{(0)}$ is outlined next, and then the Monte Carlo calculations that were used to compute P_{cc} are described.

Dilute Partition Coefficient. Except for the inclusion of a finite segment radius, the Monte Carlo approach used to determine $\Phi^{(0)}$ is identical to that described previously.[5] Briefly, a given chain was allowed to interact with any number of fibers. One end of the chain was designated as the reference or locator point, and fibers within the random matrix were labeled according to their shortest distance from that end, with "1" for the nearest neighbor, "2" for the second-nearest neighbor, and so on. Because interactions between the test chain and the various fibers are independent, it follows that

$$\Phi^{(0)} = \Phi_1\Phi_2\Phi_3... = \prod_{i=1}^{\infty}\Phi_i \quad (8)$$

That is, the dilute partition coefficient is the product of the probabilities Φ_i that a test chain will not overlap fiber i, including all fibers in the matrix, however distant. If $p(s)$ is the probability that a test chain will avoid overlap with a cylindrical fiber when one end of the chain is a dimensionless distance s from the fiber surface and $g_i(s)$ is the probability density describing

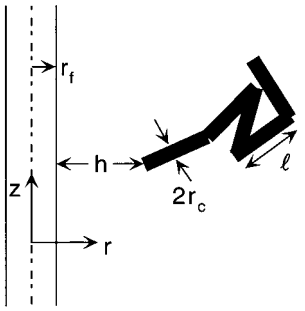

Figure 1. Computational domain used to evaluate the probability that a chain will avoid overlap with a given fiber. A chain with five segments ($n = 6$), each with length l and radius r_c, is shown with one end at a distance h from a fiber of radius r_f. Cylindrical coordinates are centered on the fiber.

the distance of the ith nearest-neighboring fiber from any point in the fibrous phase, then Φ_i is given by

$$\Phi_i = \int_0^\infty p(s)\, g_i(s)\, ds \tag{9}$$

The required probability density is[5]

$$g_i(s) = \frac{2\phi^i}{(i-1)!}(1+s)^{2i-1} \exp[-\phi(1+s)^2] \tag{10}$$

where ϕ is the volume fraction of fibers.

The computational domain used to evaluate $p(s)$ was the unbounded region external to a solid cylinder of radius r_f, with the cylinder (fiber) centered at the origin and aligned with the z axis, as shown in Figure 1. The cylindrical symmetry ensures that the probability of finding a macromolecular solute at a given position depends only on the radial coordinate, r. The dimensionless distance s was defined as h/r_f, where h is the distance of the locator end of the chain from the cylinder surface. An ensemble of chains was generated for each set of solute parameters, and the fraction of successful fits at a specified distance from the cylinder was equated with $p(s)$.

The effect of a nonzero segment radius was incorporated by modifying the algorithm used previously to detect overlap of any chain segment with a cylinder. The modified rejection criteria were tested by comparing Monte Carlo and analytical results for the partition coefficients of dilute solutions of rods of length l and radius r_c. This was done for a fiber matrix and also for a medium containing similar rods frozen in place, to test the rejection criteria for chain−fiber and chain−chain overlap, respectively. The Monte Carlo value of $\Phi^{(0)}$ was simply the recorded fraction of successful fits over many trials. The analytical results were based on the partitioning theory of Lazzara et al.[3] and the excluded volumes for finite and infinite-length rods in ref 6. The relationships between these dilute-solution partition coefficients and the respective excluded volumes are analogous to eq 5; that is, they are based on the Poisson distribution. The calculated partition coefficients are shown in Figure 2 as functions of the rod aspect ratio, l/r_c. There was excellent agreement between the Monte Carlo and analytical results for both geometries over a wide range of aspect ratios. This confirms that the rejection criteria were correctly implemented. Moreover, it shows that the Monte Carlo procedure can be used to infer excluded volumes for pairs of objects, if desired. Of importance, note that $\Phi^{(0)}$ for the medium consisting of rods can be interpreted also as P_{rr}, the probability of having no overlaps in a solution of rods. Thus, the results in Figure 2 support the use of similar Monte Carlo calculations to obtain V or P_{cc} in eq 5 (see below).

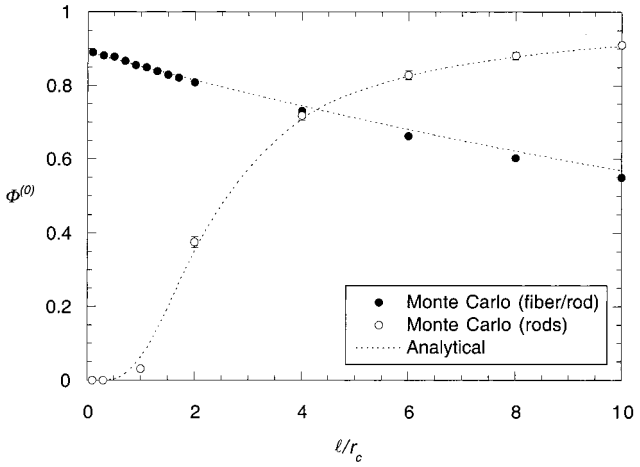

Figure 2. Partition coefficient for a dilute solution of rods of radius r_c and length l in a fiber matrix ($\phi = 0.06$, $r_c/r_f = 1/2$) or in a medium consisting of an array of like rods ($\xi = 1/3$). The Monte Carlo results are seen to agree in both cases with the analytical results from excluded-volume theory.[3,6]

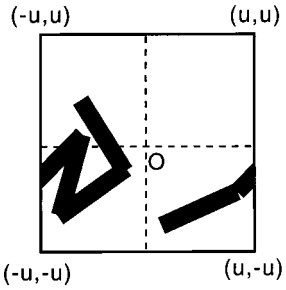

Figure 3. Schematic showing the use of periodic boundary conditions in evaluating the probability that a chain will avoid overlap with other chains in bulk solution. A chain crossing the $+u$ boundary of the control volume is shown returning at the $-u$ boundary.

The values of Φ_i were computed by evaluating the integral in eq 9 numerically using Bode's law.[9] The relative error in Φ due to the numerical integration was estimated to be <1% for all cases, which is negligible compared to the errors associated with the evaluation of $p(s)$ and with the truncation of eq 8 at a finite number of terms. The method described in Davidson et al.[10] was used to estimate the error in each of the Φ_i, and the error propagation scheme presented in Meyer[11] was used to estimate the error in Φ. Simulations with 5000 chains were sufficient to limit the absolute and relative errors in Φ to ≤ 0.01 and $\leq 8\%$, respectively (95% confidence limit). The number of terms needed in eq 8 depended on the ratio r_g/r_f and on n; as many as 90 terms were computed.

Bulk Solution Probability. A Monte Carlo method was used also to calculate P_{cc} for solutions of chains with specified number concentrations C. To do this, an ensemble of chains was generated, and the chains were positioned randomly within a cubic cell of side $2u$. Periodic boundary conditions were imposed at the cube faces to minimize edge effects, as illustrated in Figure 3. The volume of the cell was adjusted according to the desired value of C and the total number of chains used in the computation (typically 20 000). Each chain was

tested in turn to detect overlaps with any other chain, and the fraction of test chains with no overlaps was recorded. By letting each chain be a test chain, the results of many trials were obtained from each simulation. As discussed in connection with Figure 2, the fraction of chains with no overlaps is P_{cc}. The variance (σ^2) in each calculated value of P_{cc} was estimated as[11]

$$\sigma^2 = \frac{P_{cc}(1 - P_{cc})}{M} \tag{11}$$

with M being the number of chains. The estimated variances using 20 000 chains were typically low enough that, when propagated through the other calculations, they gave errors in Φ of less than 5%. Ordinarily, 20 000 chains (the limit set by the available computing resources) were sufficient to cover the desired range of C, allowing the Monte Carlo values of P_{cc} to be used directly in eq 7. Otherwise, V was estimated from the available results, and eq 5 was used to extrapolate to higher concentrations.

Experimental Methods

Agarose (type VI high gelling) and FITC-dextran of 500 and 2000 kDa molecular weights (nominal weight averages) were purchased from Sigma. Prior to use, solutions of each dextran were ultrafiltered across Biomax membranes (50 kDa nominal molecular weight cutoff, Millipore) to ensure that free fluorescein was negligible. Sols with volume fractions equal to 0.04, 0.06, or 0.08 were prepared by dissolving agarose in sodium phosphate buffer at pH 7 in an oven at 95 °C. (The volume fraction of agarose is essentially the same as its mass concentration in g/mL.[12]) The sols were allowed to gel at room temperature and then cut into disks of known volume (~30 μL), which were placed in large volumes (10 mL) of buffer containing the fluoresceinated dextran. After equilibration for 2−4 days, an aliquot (~100 μL) of each solution was collected for analysis. The gel disks were then rinsed, placed in large volumes of dextran-free buffer, and allowed to reequilibrate. Aliquots of the final solutions were collected. Dextran concentrations in the samples were measured using a spectrofluorimeter (Shimadzu) with excitation at 488 nm and emission at 515 nm. The 2−4 day equilibration periods were long compared to the characteristic times for diffusion that we calculated from the diffusivity data of Key and Sellen;[13] the calculated times ranged from 1 to 5 h for gels 170 μm in thickness.

The use of relatively large volumes allowed us to assume that (a) the dextran buffer concentration was unchanged during the first equilibration period and (b) the dextran in the buffer at the end of the second equilibration was approximately equal to the amount that had been in the gel. With these assumptions, the partition coefficient was calculated from the initial dextran concentration (C_i), the final dextran concentration (C_f), the gel volume (V_g), and the final buffer volume (V_f) as

$$\Phi = \frac{C_f V_f}{C_i V_g} \tag{12}$$

The possibility of osmotic shrinkage of agarose gels due to high external dextran concentrations was examined in a separate set of experiments. Thicknesses of gel samples with varying agarose concentrations were measured before and after the samples had been allowed to equilibrate for 2 days in buffer containing ~20 mg/mL of the 2000 kDa dextran. The thicknesses (~170 μm) were measured using a micrometer, with the gels confined gently between glass coverslips. The thickness variations were random, never exceeding 5%. This supports the assumption of constant V_g made in deriving eq 12.

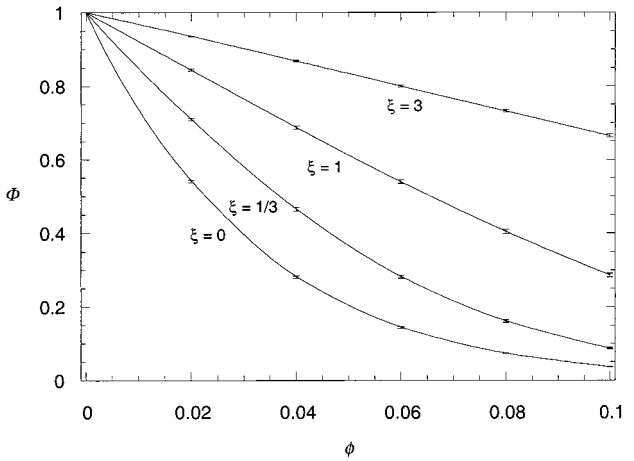

Figure 4. Theoretical effects of fiber volume fraction (ϕ) and dimensionless bulk solution concentration (ξ) on the partition coefficient (Φ). The parameters held constant are $\lambda = 5$, $n = 500$, $\beta = 115°$, and $\Lambda = 1/8$.

Results and Discussion

Theoretical Trends. In the model the partition coefficient depends on six parameters: the fiber volume fraction (ϕ), the dimensionless radius of gyration ($\lambda = r_g/r_f$), the number of mass points in the chain (n), the bond angle (β), the dimensionless segment radius ($\Lambda = r_c/r_f$), and the concentration of the chains in bulk solution. The bulk concentration was expressed relative to the critical overlap concentration (C^*), such that $\xi = C/C^*$. Critical overlap concentrations were estimated from the hexagonal close packing of solid spheres with radii equal to the radius of gyration, with the result that[14]

$$C^* = \frac{0.7404}{{}^4/_3\pi r_g^3} = \frac{0.1768}{r_g^3} \tag{13}$$

where 0.7404 is the volume fraction of spheres packed in this manner. In each plot to be presented, curves are shown for four dimensionless concentrations ($\xi = 0$, $1/3$, 1, and 3), with one other parameter varied. The remaining parameters were maintained at reference values of $\phi = 0.06$, $\lambda = 5$, $n = 500$, $\beta = 115°$, and $\Lambda = 1/8$.

Figure 4 shows the effects of fiber volume fraction. Here, as with the other theoretical plots, the error bars represent one standard deviation in the Monte Carlo results, estimated as described above. At any given bulk polymer concentration, steric exclusion of the polymer chains by the fibers caused the partition coefficient to decline monotonically with increasing ϕ, as expected. At any fixed fiber volume fraction, the partition coefficient was found to increase with bulk concentration. This effect of concentration, which was quite significant even for $\xi = 1/3$, is qualitatively similar to what has been found in other systems with solute−solute steric interactions, including rigid particles in pores,[3,15−17] rigid particles in fiber matrices,[2,3] or flexible polymers in other geometries.[4,18,19] The partition coefficient increases with concentration in each case because the steric exclusion due to other solute molecules in the bulk solution is greater than that due to solutes in the confined phase.

The effects of relative molecular size are shown in Figure 5. As one would expect, the partition coefficient declined as λ was increased, at any given ξ. However,

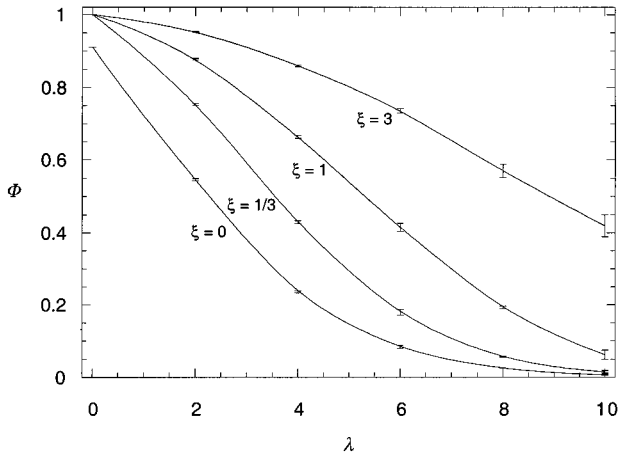

Figure 5. Theoretical effects of relative molecular size (λ) and dimensionless bulk solution concentration (ξ) on the partition coefficient (Φ). The parameters held constant are $\phi = 0.06$, $n = 500$, $\beta = 115°$, and $\Lambda = {}^1/_8$.

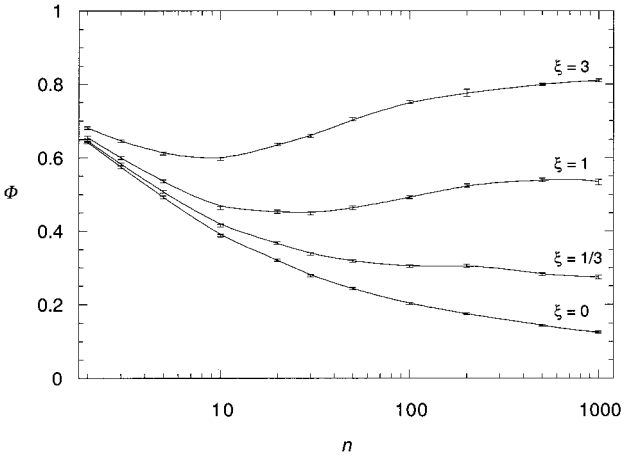

Figure 6. Theoretical effects of number of mass points (n) and dimensionless bulk solution concentration (ξ) on the partition coefficient (Φ). The parameters held constant are $\phi = 0.06$, $\lambda = 5$, $\beta = 115°$, and $\Lambda = {}^1/_8$.

careful inspection of the curves reveals that $\Phi \rightarrow 1$ as $\lambda \rightarrow 0$ for all curves with $\xi > 0$, whereas the dilute solution ($\xi = 0$) theory gives $\Phi \rightarrow 0.91$ for $\lambda \rightarrow 0$. The discrepancy in the results at small λ with $\xi \rightarrow 0$ and $\xi = 0$ is like that noted by Lazzara et al.[3] for the partitioning of concentrated solutions of spheroids in fibrous media and has the same explanation. Namely, along any curve of constant ξ, the number concentration of molecules in the bulk solution (C) increases with decreasing λ. The number concentration in the fiber matrix ($\bar{C}$) also increases, but since the partition coefficient is less than one, $\bar{C}$ increases more slowly than C. Thus, the excluded volume is increased preferentially in the bulk phase as λ decreases along a curve of constant ξ, and this is what drives the partition coefficient toward unity. In other words, the discrepancy in limiting behavior was caused by the choice of variables and constants in Figure 5, rather than by any singularity in the theory.

The next three plots examine more detailed aspects of the chain structure. Figure 6 shows the effects of the number of mass points. Whereas the partition coefficient decreased with increasing n for $\xi = 0$, as found previously,[5] the dependence on n for $\xi > 0$ was not monotonic. The nonmonotonic behavior reflects a changing balance in the competition between steric interactions in the

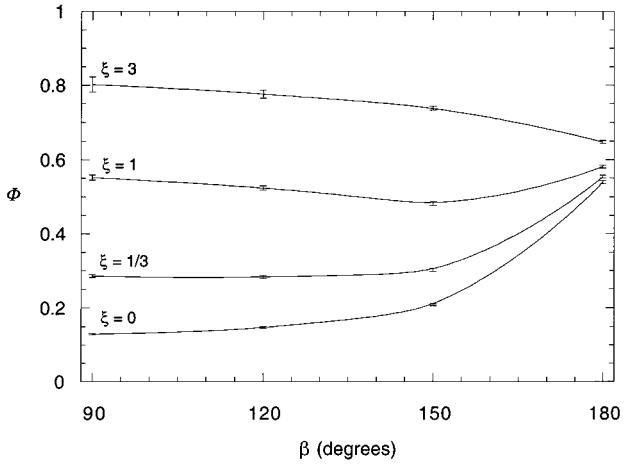

Figure 7. Theoretical effects of bond angle (β) and dimensionless bulk solution concentration (ξ) on the partition coefficient (Φ). The parameters held constant are $\phi = 0.06$, $\lambda = 5$, $n = 500$, and $\Lambda = {}^1/_8$.

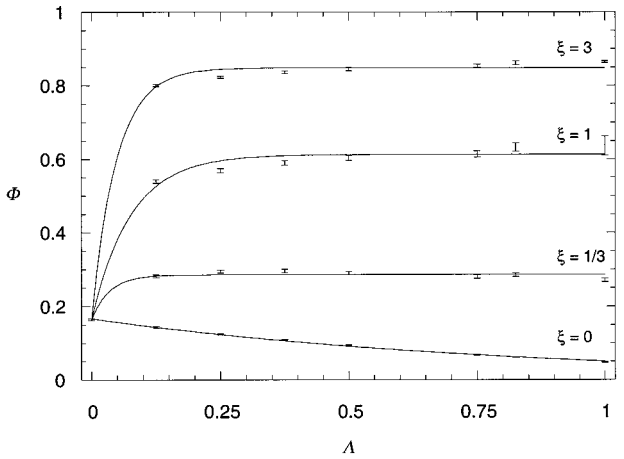

Figure 8. Theoretical effects of dimensionless segment radius (Λ) and dimensionless bulk solution concentration (ξ) on the partition coefficient (Φ). The parameters held constant are $\phi = 0.06$, $\lambda = 5$, $n = 500$, and $\beta = 115°$.

bulk solution (which tend to increase Φ) and in the fiber matrix (which tend to decrease Φ). Chain−fiber interactions tended to dominate for small n, as evidenced by the convergence of the curves. As n was increased, steric interactions among pairs of chains evidently grew much more rapidly than did those between chains and fibers. It appears that, as the chains became more coillike, additional segments tended to be found in volumes already excluded to a fiber but not yet excluded to other chains. Consequently, steric exclusion was increased preferentially in the bulk solution. For large enough numbers of mass points ($n \geq 500$), Φ was relatively insensitive to n, as shown.

Figure 7 shows the effect of the bond angle. Bond angles were restricted to $90° \leq \beta \leq 180°$ to prevent overlaps between neighboring segments. The dependence of Φ on the bond angle was found to be relatively weak for $90° \leq \beta \leq 150°$, the changes becoming significant only as rodlike conformations were approached. As shown in Figure 8, the effects of segment radius also tended to be minor, once a minimum relative radius was achieved ($\Lambda > 0.25$). As already mentioned, if the segment radius vanishes, there will be no excluded volume among chains and no effect of solute concentration; hence, all of the curves in Figure 8 converge for $\Lambda \rightarrow 0$.

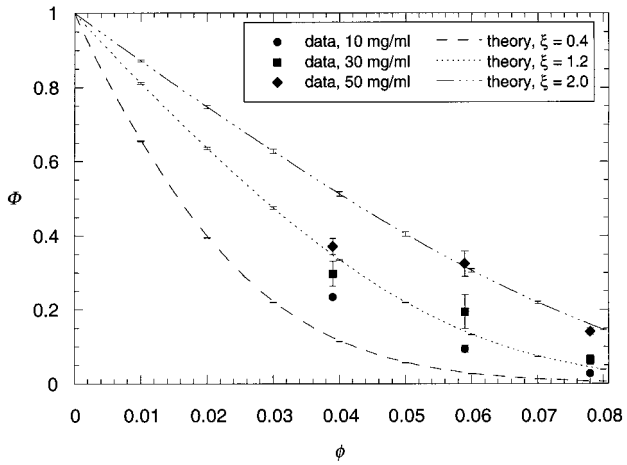

Figure 9. Measured and predicted partition coefficients of 500 kDa dextran solutions of varying concentration in agarose gels of varying volume fraction. With $r_g = 17.6$ nm (based on M_w), $\lambda = 9.3$ and dextran concentrations of 10, 30, and 50 mg/mL correspond to $\xi = 0.40$, 1.2, and 2.0, respectively. The error bars for the data and Monte Carlo calculations each represent one standard deviation.

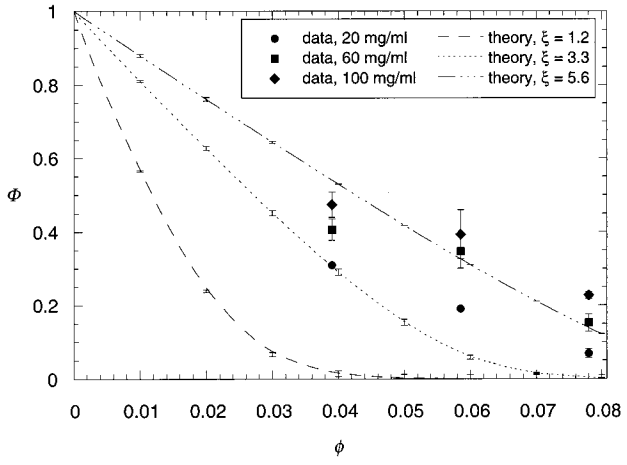

Figure 10. Measured and predicted partition coefficients of 2000 kDa dextran solutions of varying concentration in agarose gels of varying volume fraction. With $r_g = 32.0$ nm (based on M_w), $\lambda = 17$ and dextran concentrations of 20, 60, and 100 mg/mL correspond to $\xi = 1.2$, 3.3, and 5.6, respectively. The error bars for the data and Monte Carlo calculations each represent one standard deviation.

Figures 6−8 show that the partition coefficient is insensitive to the details of the chain structure when n is large and β and Λ are moderate. This suggests that, for these conditions, Φ can be considered a function primarily of λ, ϕ, and ξ. The Monte Carlo results for $n \geq 500$, $90° \leq \beta \leq 150°$, and $0.25 \leq \Lambda \leq 1$ are well represented by the following empirical formula:

$$\Phi = \frac{\exp[-(1 + \pi^{9/8}\lambda^{4/3})\phi]}{\left[\exp\left(-\frac{\pi^2}{2}\lambda^{-5/16}\xi\right)\right]^{1-\Phi}} \qquad (14)$$

Comparing this with eq 7, it is seen that the numerator is $\Phi^{(0)}$ and the bracketed term in the denominator is P_{cc}. The absolute and relative root-mean-square (rms) errors in eq 14 were 0.03 and 30%, respectively. The relatively large percentage error is due mainly to the discrepancies between eq 14 and the $\xi = 0$ results in Figure 8 (i.e., the effect of segment radius in dilute solutions); without those results, the relative rms error is reduced to 8%.

Partitioning of Dextran in Agarose. The partition coefficients measured for dextrans of nominal molecular weights 500 and 2000 kDa in agarose gels are shown in Figures 9 and 10, respectively. For a fixed bulk concentration of either size dextran, Φ decreased as ϕ was increased. That is, increasing the volume fraction of agarose fibrils increased the steric exclusion of dextran molecules from the gel, consistent with expectations from Figure 4. For any given combination of dextran size and agarose volume fraction, the partition coefficient increased with increasing dextran concentration, again in qualitative agreement with the theoretical predictions. The sensitivity of Φ to dextran concentration was greater at the higher agarose concentrations (i.e., when Φ was smallest). For the range of dextran concentrations examined, the ratio of Φ at the highest dextran concentration to that at the lowest ranged from 1.5 to 1.6 at $\phi = 0.04$ to 3.3−5.2 at $\phi = 0.08$, depending on the dextran size. Thus, the data confirm that the partition coefficient of a flexible polymer can be affected markedly by its bulk solution concentration.

Table 1. Parameter Values Used for Dextran[a]

M_d (kDa)	r_g (nm)	r_c (nm)	β (deg)	n	ρ_d* (mg/mL)	ξ
500	17.6	0.27	116	500	25	0.40−2.0
2000	32.0	0.27	116	1000	18	1.1−5.6

[a] See text for sources for parameter values.

Quantitative comparisons with the theory require estimates of the parameters that characterize agarose and dextran. The agarose fiber radius was taken to be $r_f = 1.9$ nm, which is the number-average of fiber radii reported by Djabourov et al.[20] The values used for the two dextran sizes are summarized in Table 1. The radii of gyration for dextrans measured by Nordmeier et al.[21] are correlated well by a power-law dependence on molecular weight. The estimated r_g values for 500 and 2000 kDa are 17.6 and 32.0 nm, respectively. The segment radius was estimated by modeling the dextran chain as a cylinder of uniform radius, with a length equal to the contour length of the molecule and a volume based on the specific volume reported for dextran, which is 0.61 mL/g.[22] The contour length was obtained by multiplying the degree of polymerization by the monomer length, which was taken to be 1.0 nm.[23] The resulting segment radius was $r_c = 0.27$ nm. The bond angle between monomers was reported by Arnott and Scott[23] as $\beta = 116°$. The number of mass points was set somewhat arbitrarily at $n = 500$ for 500 kDa dextran and $n = 1000$ for 2000 kDa dextran. (Using $n = 2000$ for the larger dextran would have been more consistent, but very tedious computationally and not very informative; as shown in Figure 6, the predicted values of Φ were quite insensitive to n for $n > 500$.) The values of n used were much less than the degrees of polymerization (2035 for 500 kDa dextran, 8771 for 2000 kDa dextran). The critical overlap concentrations computed from eq 13, expressed in mass units ($\rho_d^* = C_d^* M_d$, where M_d is molecular weight), were 25 and 18 mg/mL for the 500 and 2000 kDa dextrans, respectively. Dividing these values into the respective experimental concentrations of 10−50 and 20−100 mg/mL, the dimensionless concentrations were calculated to be $\xi = 0.40$−2.0 for the smaller dextran and $\xi = 1.1$−5.6 for the larger

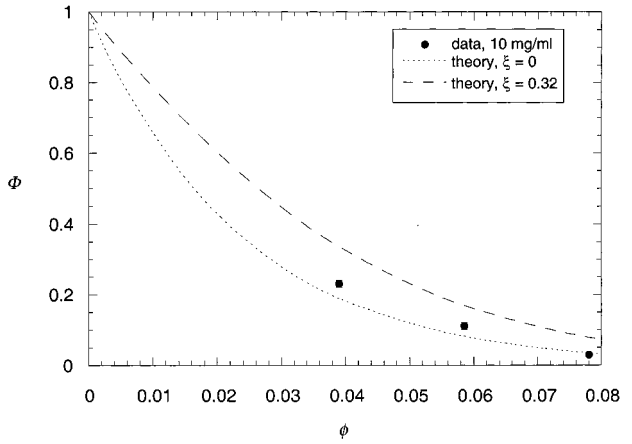

Figure 11. Measured and predicted partition coefficients of 500 kDa dextran in agarose gels of varying volume fraction. With $r_g = 12.0$ nm (based on M_n), $\lambda = 6.3$ and the dextran concentration of 10 mg/mL corresponds to $\xi = 0.32$. The theoretical curves are from eq 14 with $\xi = 0$ or $\xi = 0.32$.

one. As shown in Figures 9 and 10, quantitative agreement between the predictions and data was reasonably good at the higher dextran concentrations (i.e., at $\xi =$ 1.2 and 2.0 for 500 kDa and $\xi = 5.6$ for 2000 kDa). In the more dilute solutions, however, the computed values of Φ fell well below those measured.

A factor that undoubtedly influenced the results is the polydispersity of the commercial dextran preparations. Because it was impractical to compute excluded volumes for each of the many possible combinations of unlike chains, the effects of polydispersity could be quantified only for dilute solutions. Fortuitously, this situation is particularly interesting, because the largest discrepancies between the predicted and measured partition coefficients occurred at the lowest dextran concentrations. We focused on the 500 kDa dextran at the lowest concentration, because that most closely approximated a dilute solution (i.e., ξ was smallest). As described in the Appendix, it was estimated that $M_w/M_n = 2.7$ for that dextran, where M_w and M_n are the weight-averaged and number-averaged molecular weights, respectively. Taking into account the calculated distribution of molecular weights, the partition coefficient computed for the mixture was found to be similar to that for a dextran with molecular weight equal to M_n; details are in the Appendix. This suggests that it would be more appropriate to base dilute-solution predictions on M_n than on M_w (which was used in Figures 9 and 10). Accordingly, predictions were made by using $r_g = 12.0$ nm (corresponding to $M_n = 184$ kDa) in eq 14. Curves were computed for the dilute limit ($\xi = 0$) and for the experimental dextran concentration ($\xi = 0.32$); the former neglects solute−solute interactions, and the latter approximates them as if they were occurring among like chains. As shown in Figure 11, the agreement of either curve with the data was quite good for all three agarose concentrations. Thus, for relatively dilute solutions of the 500 kDa dextran, the partition coefficient of the mixture was predicted much better by using M_n than by using M_w. The extent to which this might be true for dilute solutions of other polydisperse polymers, or for concentrated solutions, is not known. However, the relatively accurate predictions at high concentrations (Figures 9 and 10) suggest that polydispersity may be less important under those conditions.

A factor not considered in our model is solvent quality. In good solvents, linear polymers will tend to have more expanded conformations than those computed here, for a given combination of bond angle, monomer length, and degree of polymerization. More expanded conformations would result also if intramolecular steric interactions were not neglected, as done here. However, the use of measured values of r_g, as in the dextran comparisons, should at least partially compensate for these omissions. Another limitation that should be mentioned is that, as in previous theories for partitioning in fiber matrices,[1−3,5] overlap of the fibers may occur. A consequence of the shared volume is that the nominal value of the fiber volume fraction (based on fiber length per unit volume) will somewhat exceed the actual volume fraction.[3] Similarly, there is some overlap of the polymer chains in the concentrated bulk solutions generated to compute P_{cc}.

Conclusion. A theory was developed to describe the equilibrium partitioning of concentrated solutions of flexible, linear polymers in fibrous membranes and gels. In this theory the fibrous material or gel is characterized by two parameters, the fiber radius and fiber volume fraction, and the polymeric solutes are described by a radius of gyration, a number of mass points per chain, a bond angle, and a segment radius. Although the fibrous material and flexible polymer were each represented very simply, and only steric interactions were considered, the theory was found to be fairly successful in predicting experimental values of partition coefficients.

Acknowledgment. This work was supported by Grant DK20368 from the National Institutes of Health. J.A.W. is the recipient of a National Science Foundation Graduate Fellowship.

Appendix

Weight-averaged and number-averaged molecular weights for dextrans sold by Sigma were measured by Ioan et al.[24] An exponential least-squares fit to their data yielded $M_n = 184$ kDa for $M_w = 500$ kDa, or a polydispersity index for our smaller dextran of $M_w/M_n = 2.7$. To predict the observed partition coefficients for such a sample, a probability distribution for molecular weight is needed. That probability distribution was computed using the results of Erlander and French,[25] which are applicable to polymers with branched structures, such as dextran. Their formulation assumes that each monomer possesses f reactive groups. One of the groups on a given monomer (denoted as A) can react with any of the remaining $f-1$ groups (denoted as B_i) on another monomer, but not with A groups. Reactions within the same monomer are not allowed. Dextran monomers (α-D-glucopyranosyl residues) are connected primarily by 1−6 linkages, but a small number also have 1−4 linkages. Accordingly, dextran has groups designated as A, B_1, and B_2, and $f = 3$. The probability that a given chain has x monomer units is

$$P(x) = \frac{1}{x}\sum_{b_2=0}^{x-b_1}\sum_{b_1=0}^{x}\prod_{i=1}^{2}\binom{x}{b_i}p_i^{b_i}(1-p_i)^{x-b_i} \qquad \text{(A1)}$$

where b_i is the number of $A-B_i$ bonds in the chain and p_i is the probability that a given monomer has such a bond. The number-averaged (x_n) and weight-averaged

Table 2. Theoretical Partition Coefficients for Dilute Solutions of 500 kDa Dextran in Agarose[a]

ϕ	$\langle\Phi\rangle$	$\Phi(M_w)$	$\Phi(M_n)$
0.04	0.13	0.062	0.19
0.08	0.034	0.0038	0.035

[a] The partition coefficients are: $\langle\Phi\rangle$, the observable value for the mixture; $\Phi(M_w)$, the value for a dextran with a molecular weight equal to the mixture weight average; $\Phi(M_n)$, the value for a dextran with a molecular weight equal to the mixture number average.

(x_w) degrees of polymerization are related to the bond probabilities by

$$x_n = \frac{1}{1 - p_1 - p_2} \tag{A2}$$

$$x_w = \frac{1 - (p_1^2 + p_2^2)}{(1 - p_1 - p_2)^2} \tag{A3}$$

Thus, the p_i values can be calculated from measurements of M_n and M_w. With $M_n = 184$ kDa, $M_w = 500$ kDa, and a monomer of 114 Da, we found that $p_1 = 0.99915$ and $p_2 = 0.00023$.

Because the fluorescence of FITC-dextran is proportional to molecular weight,[26] the measured partition coefficients for the polydisperse samples were weight-averaged values. Accordingly, the theoretical partition coefficient for the mixture was calculated as

$$\langle\Phi\rangle = \int_0^\infty w(x)\,\Phi(x)\,dx \tag{A4}$$

where the weight fraction of chains with x monomers is given by

$$w(x) = \frac{xP(x)}{x_n} \tag{A5}$$

Partition coefficients for each molecular size were obtained from eq 14 with $\xi = 0$. For consistency with the parameter values in Table 1, the relative molecular size (λ) in these calculations was estimated using the r_g values from Nordmeier,[21] which are about 10% smaller than those of Ioan et al.[24] As shown in Table 2, $\langle\Phi\rangle$ corresponded better to that for a monodisperse dextran with a molecular weight equal to M_n than to that for a monodisperse dextran with a molecular weight equal to M_w, especially at the higher agarose concentration. This suggests that, for dilute solutions of the 500 kDa dextran, predictions using M_n should be more accurate than those using M_w. This conclusion might not apply to partition coefficients measured for other polydisperse polymers or even for concentrated solutions of this particular dextran.

References and Notes

(1) Ogston, A. G. *Trans. Faraday Soc.* **1958**, *54*, 1754.
(2) Fanti, L. A.; Glandt, E. D. *J. Colloid Interface Sci.* **1990**, *135*, 385, 396.
(3) Lazzara, M. J.; Blankschtein, D.; Deen, W. M. *J. Colloid Interface Sci.* **2000**, *226*, 112.
(4) Thompson, A. P.; Glandt, E. D. *Macromolecules* **1996**, *29*, 4314.
(5) White, J. A.; Deen, W. M. *Macromolecules* **2000**, *33*, 8504.
(6) Jansons, K. M.; Phillips, C. G. *J. Colloid Interface Sci.* **1990**, *137*, 75.
(7) Flory, P. J. *Principles of Polymer Chemistry*; Cornell University Press: Ithaca, NY, 1953; pp 415, 430.
(8) Giddings, J. C.; Kucera, E.; Russell, C. P.; Myers, M. N. *J. Phys. Chem.* **1968**, *72*, 4397.
(9) Press, W. H.; Flannery, B. P.; Teukolsky, S. A.; Vetterling, W. T. *Numerical Recipes in Fortran*, 2nd ed.; Cambridge University Press: Cambridge, UK, 1986; pp 272−273, 838−842.
(10) Davidson, M. G.; Suter, U. W.; Deen, W. M. *Macromolecules* **1987**, *20*, 1141.
(11) Meyer, P. L. *Introduction to Probability and Statistical Applications*; Addison-Wesley Publishing: Reading, MA, 1965; p 149.
(12) Johnson, E. M.; Berk, D. A.; Jain, R. K.; Deen, W. M. *Biophys. J.* **1995**, *68*, 1561.
(13) Key, P. Y.; Sellen, D. B. *J. Polym. Sci., Polym. Phys. Ed.* **1982**, *20*, 659.
(14) Wolff, C. *Eur. Polym. J.* **1977**, *13*, 1739.
(15) Anderson, J. L.; Brannon, J. H. *J. Polym. Sci., Polym. Phys. Ed.* **1981**, *19*, 405.
(16) Glandt, E. D. *AIChE J.* **1981**, *27*, 51.
(17) Chun, M.-S.; Phillips, R. J. *AIChE J.* **1997**, *43*, 1194.
(18) Bleha, T.; Cifra, P.; Karasz, F. E. *Polymer* **1990**, *31*, 1321.
(19) Wang, Y. M.; Teraoka, I. *Macromolecules* **1997**, *30*, 8473.
(20) Djabourov, M.; Clark, A. H.; Rowlands, D. W.; Ross-Murphy, S. B. *Macromolecules* **1989**, *22*, 180.
(21) Nordmeier, E. *J. Phys. Chem.* **1993**, *97*, 5770.
(22) Bohrer, M. P.; Deen, W. M.; Robertson, C. R.; Troy, J. L.; Brenner, B. M. *J. Gen. Physiol.* **1979**, *74*, 583.
(23) Arnott, S.; Scott, W. E. *J. Chem. Soc., Perkin Trans.* **1972**, *2*, 324.
(24) Ioan, C. E.; Aberle, T.; Burchard, W. *Macromolecules* **2000**, *33*, 5730.
(25) Erlander, S.; French, D. *J. Polym. Sci.* **1956**, *20*, 7.
(26) Schröder, U.; Arfors, K.-E.; Tangen, O. *Microvasc. Res.* **1976**, *11*, 33.

MA0022046